

Abstract

Research has been done to investigate the growth of nanoparticles in the Pulsed Laser Deposition (PLD) process. Several groups succeeded in the creation of nanoparticles, all using different materials for different applications. The main goal of this research is not to produce nanoparticles of a certain material but to look into the process of formation of nanoparticles. In this work platinum (Pt) is used as a model system since stacked platinum nanoparticles might be used as a porous conducting electrode. A stack of nanoparticles combines the porosity of the stacked particles, making them gas permeable, with the conductivity of platinum. These electrodes might find an application in the near future in thin-film oxygen sensors.

The formation of nanoparticles is highly dependant on the kinetics of the ablated species in the plasma. The implementation of an ion probe is therefore useful since probe measurements reveal ion energies. In this work the ability to use this probe for the indication of the correct regime for nanoparticle formation has been investigated.

Several problems had to be overcome, mainly concerning the analysis of these particles. Atomic Force Microscopy (AFM) is rather difficult since there hardly is any interaction between the surface and the particles, causing the particles to move during analysis. Oxidation of the films caused problems for Scanning Electron Microscopy (SEM).

This work showed promising results in the creation of platinum nanoparticles by Pulsed Laser Deposition. The probe gave interesting results for better understanding of particle kinetics in laser-induced plasmas, although the probe turned out not to be effective in the prediction of the nanoparticle growth regime.

Table of Contents

Abstract	1
Table of Contents	2
List of Used Abbreviations and Symbols	3
Chapter 1 Introduction	4
Why nano?	4
Which technique?	4
Model system	4
Organization of the report	4
Chapter 2 Experimental Methods	5
2.1 Pulsed Laser Deposition	5
2.2 Atomic Force Microscopy (AFM)	5
2.3 Scanning Electron Microscopy (SEM)	6
2.4 Silicon substrates	7
Chapter 3 Ion Probe Diagnostics	8
3.1 Theory	8
3.2 Experimental	10
3.3 Results	11
3.4 Discussion	15
3.5 Conclusion	15
Chapter 4 Platinum Nanoparticles	16
4.1 Theory	16
4.2 Experimental	18
4.2.1 The influence of target-substrate separation	18
4.2.2 Influence of the ambient gas pressure	20
4.2.3 Influence of spot size and spot geometry	21
4.2.4 Influence of the laser repetition rate	22
4.2.5 Influence of the deposition time/number of pulses	23
4.3 Deterioration of Pt-nanoparticle films	25
4.4 Discussion	26
4.5 Conclusions	26
General Discussion and Conclusions	27
Dankwoord	28
Literature	29

List of Used Abbreviations and Symbols

σ	surface tension
θ	deposition angle
$\Delta\mu$	supersaturation
ϵ_0	permittivity of vacuum
ϵ_c	dielectric constant
AFM	Atomic Force Microscopy
Ar	Argon
Au	Gold
CM	Contact Mode
COM	Center of Mass
G	Gibbs free energy
KE_{avg}	Average Kinetic Energy
KrF	Krypton Fluor
M	particle mass
MB	Maxwell Boltzmann
n	atom number density
N	Nitrogen
O	Oxygen
PLD	Pulsed Laser Deposition
Pt	Platinum
R	Gas constant (8,3145 J mol ⁻¹ K ⁻¹)
r	radius
R'	deposition rate
R ₀	equilibrium deposition rate
r _a	radius of jacketed ion
RT	Room Temperature
SEM	Scanning Electron Microscopy
Si	Silicon
T	Gas temperature
TM	Tapping Mode
TOF	Time of Flight
v	Particle velocity
v ₀	Center Of Mass velocity
v _p	Peak velocity
v _{rms}	Root Mean Square velocity

Chapter 1 Introduction

Why nano?

Over the years dimensions of structures have shifted to smaller sizes. The dimensions went from milli- to micro- to nanometers. The last step towards nanometer-size structures wasn't only a huge technological challenge but also a scientific one. Many material properties of these nano-sized materials start to deviate from their bulk properties. An interesting example is the change of the photoluminescence band in silicon consisting of small particles as compared to normal silicon as a result of a kind of quantum confinement effect ^[1]. Physical properties can be tuned by controlling the particle size ^[2], which make these particles interesting for applications. It is also possible to combine advantages of materials and nanometer-sized structures. Combining the porosity of stacked nanoparticles and the good conductance of a noble metal like platinum results in extremely porous conducting electrodes. A description of the growth dynamics will be of great importance for the control of the particle size.

Which technique?

A complete other deposition regime in parameter space is needed for the formation of nanoparticles compared to thin film growth. High particle energies and low number densities during deposition will prevent particle growth. On the other side, high supersaturation ratios can cause homogeneous- or self-nucleation resulting in particles. Pulsed Laser Deposition (PLD) seems to be the most promising deposition technique for this research since high supersaturation ratios can be obtained and particle energies can be tuned. Also its broad range of deposition parameters makes PLD interesting for growth studies. Ion probe measurements have also been performed since there are many parameters influencing particle formation and complete depositions are time consuming. These "fast" ion probe results might be linked to nanoparticle formation and speed up the research.

Model system

In this research platinum nanoparticle formation by PLD is chosen as a model system. As mentioned earlier platinum nanoparticles are interesting for the creation of porous electrodes. These electrodes can find their application in the near future in oxygen or NO_x gas sensors.

So, the final goal of this project is to obtain a description of the nanoparticle formation process during PLD and investigating the possibility to link probe-measurements to particle formation.

Organization of the report

This report will treat the following subjects in the following order

- Chapter 2 *Experimental methods*, this chapter describes the different techniques used for the creation of nanoparticles and the analysis
- Chapter 3 *Ion-probe diagnostics*, this chapter will treat the theory used to do Langmuir ion probe diagnostics. It also reflects the experimental results
- Chapter 4 *Platinum nanoparticles*, this chapter discusses the experiments done to obtain nanoparticles and how to tune their size
- Chapter 5 *Discussion and conclusion*, about the obtained results and about the combination ion probe/particle formation

Chapter 2 *Experimental Methods*

2.1 Pulsed Laser Deposition

Pulsed Laser Deposition [3] is used in many different types of research, mostly for the preparation of thin films. PLD has several advantages over other deposition techniques of which for this research most important is the high degree of supersaturation obtained during deposition. Another advantage for growth kinetics studies is the ability to control the deposition parameters independently over a broad range. A schematic view of a PLD setup is shown in figure 2.1.

The system consists of a vacuum chamber in which a rotating target is mounted. A Lambda Physik KrF laser is the external energy source for the deposition. The laser beam has a wavelength of 248 nm, a pulse energy of around 650 mJ and a pulse duration of about 20 ns. The vacuum in the deposition chamber has to be broken after each run since the system is not equipped with a load-lock. Ion probes or substrate can be moved around 3 dimensions in the chamber to align it in the plasma and adjust the target-substrate separation.

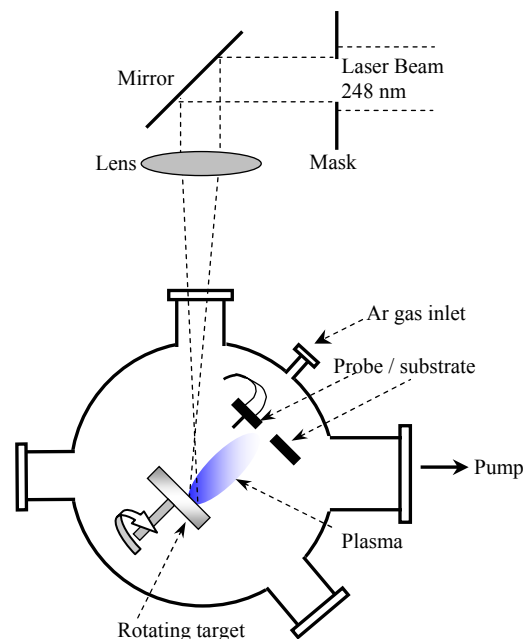


Figure 2.1: Schematic view of a PLD system

The laser beam passes through a mask to give it the correct size and geometry and is focussed by a lens on the target. The target material is evaporated in the first few nanoseconds and this vapour is heated up further in the remaining pulse duration, creating the plasma. Driven by the pressure gradient, this plasma is subsequently expanding, converting thermal energy into kinetic energy. The plasma is cooled down and species decelerated by the ambient gas followed by deposition on a substrate.

Replacing the normal heater equipped with a substrate by an altered heater equipped with an ion probe enables easy switching between deposition on a substrate and plasma characterisation, without changing the deposition geometry significantly.

2.2 Atomic Force Microscopy (AFM)

Contact Mode (CM) and Tapping Mode (TM) Atomic Force Microscopy was performed by a Digital Instruments NanoScope IV microscope. A small cantilever with a tip is scanned across a surface while the sample is moved up and down to maintain a constant force on the tip. This movement in height of the sample is then transferred into an image.

AFM is the best candidate for nanoparticle characterisation because of its high vertical resolution. Since the horizontal resolution of the AFM is depending on the tip geometry, particle sizes can best be obtained by measuring their height. If the particles are truly spherical, height information obtained from an AFM image will give the exact particle diameter. It should be noted that particles could be deformed at the impact with the substrate. Particle size comparison between images can be done when series are made, however care should be taken because tip geometries can change during usage.

An AFM image also indicates if particles are formed in the gas phase or at the substrate. Provided the film is thick enough, the image reflects an agglomeration of particles in the case of substrate growth or a “stack” of spheres as a result of gas phase growth. An extensive description about particle growth is given in the next chapter. An example is given in figure 2.2.

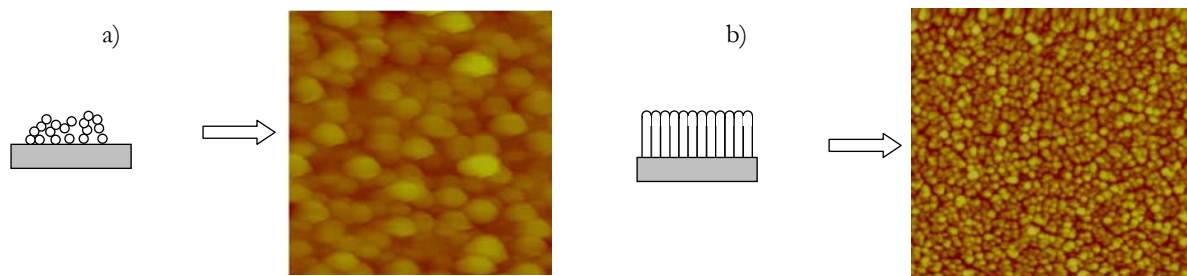


Figure 2.2: AFM images made from samples representing a) gas phase particle growth and b) (columnar) substrate growth. Both images are $1 \times 1 \mu\text{m}$, a) has a data-scale of 150 nm and b) 25 nm

In figure 2.2 a) particles can be distinguished that are covered partly by overhead species. In figure 2.2 b) particles consist of columns densely packed forming larger grains. These grains are separated by a gap also visible in this image.

Although the interaction forces are kept as low as possible, still particles were picked up or just pushed forward by the AFM-tip, especially in the case of gas-phase particle growth. Brittle surfaces with step edges > 50 nm are very hard to analyse by AFM. A thin layer of gold (< 15 nm), put on primarily for SEM image improvement, fixes these particles and enables AFM-imaging. Analysis of the DC-sputtered layer of gold (Au) showed some structures but these are negligibly small compared to nanoparticle structures (see paragraph 2.4). Still particle sizes can be measured since the relative height of the particles is not changed, shown in figure 2.3.

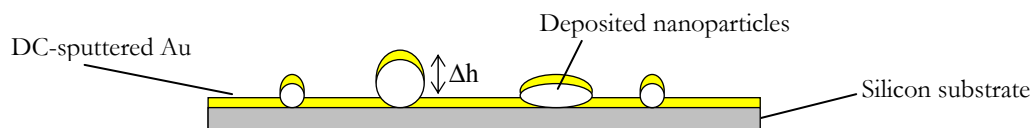


Figure 2.3: Substrate with different shapes of particles on top. The sputtered gold layer does not influence measured heights.

2.3 Scanning Electron Microscopy (SEM)

Another useful technique in sample analysis is Scanning Electron Microscopy. In this research a JEOL 5610 SEM is used. A beam of electrons drawn from a filament is scanned over the surface of the sample. The secondary electrons emitted from the surface are recorded by a detector and converted into an image.

SEM is mainly used to proof that the gas phase nanoparticle formation regime has started. Cross-section images were made at the edge of a broken sample at a 45° angle. This reveals either columns or particles. SEM has another advantage over AFM. There is no contact at all with the surface of the sample. Although in AFM the forces are very small (< 10 nN), the interaction may be enough to destroy the surface since the particles are often loosely stacked

SEM is not easily done since the depositions were done on oxidized silicon substrates. Charging of the surface is the main problem especially when the substrates are not completely covered with platinum. Sputter deposition of a thin layer of gold (8-15 nm) on the samples highly improved the quality.

2.4 Silicon substrates

In gas-phase nanoparticle formation research the influence of the substrate should be kept as small as possible. The only requirement for the substrate is that it should be flat for accurate particle size analysis. Ultrasonically cleaned silicon meets these requirements. 10x10 mm silicon substrates are carved with a pen with a diamond tip and broken into 5x5 mm substrates. Before further cleaning the substrates are carefully rinsed with ethanol to prevent scratching by any fragments left from cutting. All substrates are cleaned first for 15 minutes in acetone then rinsed with demi-water followed by 15 minutes of cleaning in ethanol. Finally the samples are dried with nitrogen. Removal of the oxide layer is not necessary since AFM-obtained rms-values are in the order of 0.1 nm (peak height ~ 1 nm). Figure 2.4 a) shows an AFM-image of cut and cleaned silicon substrate.

It is important to know the morphology of this deposited film since if the Au film consists of nanoparticles itself it will not be useful. 20 nm of gold was DC-sputtered on silicon and analysed by AFM. The results are shown in figure 2.4 b). It is clear that the rms-value is increased slightly but the dimensions of the observed structures in figure 2.4 b) are much smaller than the particles created in this research.

Deposition of gold on top of the nanoparticles was done to improve the ability to perform SEM. It was also investigated if the sputter deposition of gold before the deposition of nanoparticles could be used for the creation of conducting substrates for better SEM results. The quality of the SEM images did not improve by introducing this conducting layer.

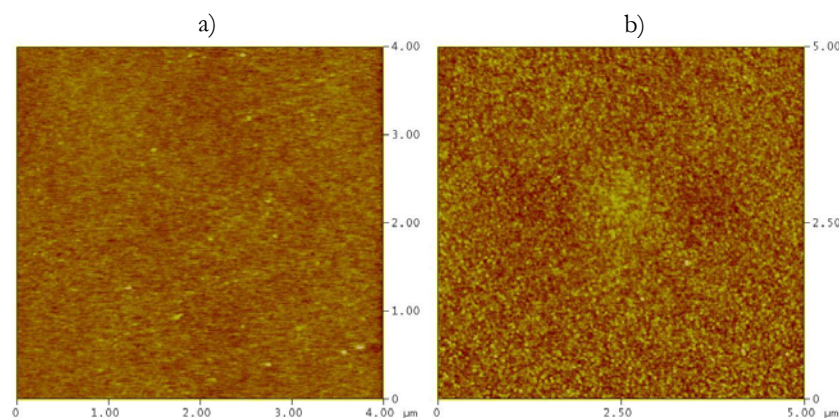


Figure 2.4: *AFM image of*

a) cleaned silicon substrate, rms = 0.073 nm, peak height = 1.8 nm

b) cleaned silicon with 20 nm DC-sputtered Au, rms = 0.15 nm, peak height = 1.66 nm

Chapter 3 Ion Probe Diagnostics

Gas-phase nanoparticle formation depends heavily on the supersaturation and the kinetic energy of the ablated species in the plasma. Since Langmuir probes are able to reveal particle energies, probe measurements can be very useful in nanoparticle formation research. Values for particle energies and other quantities measured by simple ion probes have to be taken with a pinch of salt. The many assumptions necessary made for probe measurements make them deviate from the proper values. Nevertheless, a complete set of measurements might predict the right regime for nanoparticle formation. Time-consuming experiments can be replaced by fast probe measurements to scan the complete parameter space.

Most of the existing theory about probe diagnostics in plasmas is for DC plasmas. Little work is on time-varying plasmas like RF plasmas [4]. A complete theoretical description for probe diagnostics in PLD plasmas was not found [5][6] in literature. One of the first assumptions made is that the amount of ions collected by the probe is not depending on the energy; all ion-energies are equally collected. In this research where deposition is studied with the probe, the probe tip conducting area is altered during deposition and the probe becomes completely ineffective when depositing insulating materials [7].

3.1 Theory

After the plasma has formed it starts to expand into the chamber. While expanding, the thermal energy of the particles in the plasma will be transformed into kinetic energy. If the emission is truly thermal at low number densities, the emitted particles will disperse without collisions and the velocity distribution has the form of a “half range” Maxwellian [8]. This means that particle velocities only have positive values normal to the surface of the target material and the angular distribution is of the form $\cos(\theta)$. This is not the case for a laser created plasma. The number densities are higher and the velocity distribution is altered to a “full range” Maxwellian *in a center of mass (COM) coordinate system*. The emission shows strong forward peaking ($\cos^n(\theta)$), leading to significant recondensation. In a few mean free path lengths ($< 1\mu\text{m}$ for the high pressures obtained in a newly created plasma) of the target surface the plasma develops from a velocity distribution with only positive values to a “full range” Maxwellian plasma. This development region is called the *Knudsen layer* and the process is a highly non-equilibrium collision process. As few as 3 collisions per particle is enough to form this Knudsen layer, which occurs essentially in 1.5 mean free paths [8].

A Maxwell-Boltzmann (MB) velocity distribution has the form of the following expression,

$$f(v) = 4\pi \left[\frac{M}{2\pi RT} \right]^{\frac{3}{2}} v^2 e^{-\frac{Mv^2}{2RT}}, \quad (3.1)$$

where M is the particle mass, T the gas temperature, R the gas constant and v is the particle velocity. The general shape of the MB distribution is shown in figure 3.1.

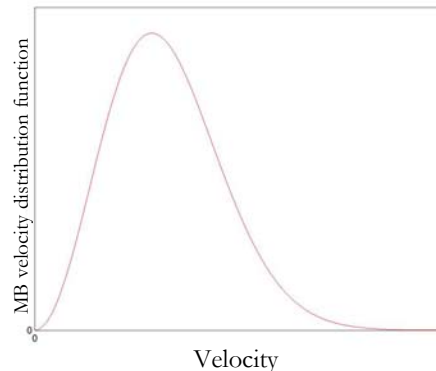


Figure 3.1: Shape of a fully developed Maxwell Boltzmann velocity distribution

Since the plasma has a Maxwellian velocity distribution with a center-of-mass velocity (v_0), equation (3.1) becomes,

$$f(v) = 4\pi \left[\frac{M}{2\pi RT} \right]^{\frac{3}{2}} (v-v_0)^2 e^{-\frac{M(v-v_0)^2}{2RT}}, \quad (3.2)$$

to include this COM-velocity. To make the fit with experimental results equation (3.2) can be rewritten into,

$$f_{fit}(v) = sC(a^{\frac{3}{2}})(v-v_0)^2 e^{-a(v-v_0)^2}, \quad (3.3)$$

with $a=M/2RT$ being the main fitting parameter. This parameter fixes the width of the distribution. $C=4\pi^{1/2}$ while s is the fitting parameter for the height of the curve. The height of the probe signal depends on the amount of ions collected by the probe. This amount of ions is lowered as, for example, a function of distance. As distance increases, the number of ions decreases because of ion-electron recombination and since the plasma is three dimensionally expanding. A Maxwell-Boltzmann distribution has two important characteristic velocities,

$$\begin{aligned} v_p &= \sqrt{\frac{2RT}{M}} \\ v_{rms} &= \sqrt{\frac{3RT}{M}} \end{aligned} \quad (3.4)$$

in which v_p is the most probable speed (maximum of the distribution function) and v_{rms} is the root-mean-square velocity. v_{rms} is related to the kinetic energy of the gas,

$$KE_{avg} = \frac{1}{2} m v_{rms}^2 = \frac{3m}{4a} \quad (3.5)$$

So a value for the energy of the plasma can be obtained by fitting a MB-distribution to the measured time-of-flight (TOF) curves.

3.2 Experimental

In this research, the simplest version of a Langmuir probe is chosen. This is a cylindrical (or wire) probe consisting of a piece of stripped coaxial cable. Its operation depends on the collection of charged particles, in our case ions. The tip is biased at a voltage of -30V and immersed into the laser-produced plasma. This potential is enough to repel most of the electrons but does not disturb the plasma plume significantly. The ion current is converted into a voltage by a simple electric circuit and is transferred to an oscilloscope. The result is a (TOF) curve, which contains information about the energy of the ions.

A picture and a schematic view of the probe set up is shown in figure 3.2. The probe consists of a heater with a hole drilled in the middle and the end of a coaxial cable sticking out of it. A gold plated tip is soldered on the wire on which the ions are collected. This tip is 9 mm long and has a 1.5 mm diameter. The ion current is transported through the core of the coaxial cable while the outer shield remains grounded. The distance d (target-tip, fig. 3.2 b)) can be varied or the heater can be completely removed. By changing the distance s (tip-heater, fig. 3.2 b)) the difference in ion energy at the substrate and the ion energy of the free expanding plasma can be investigated.

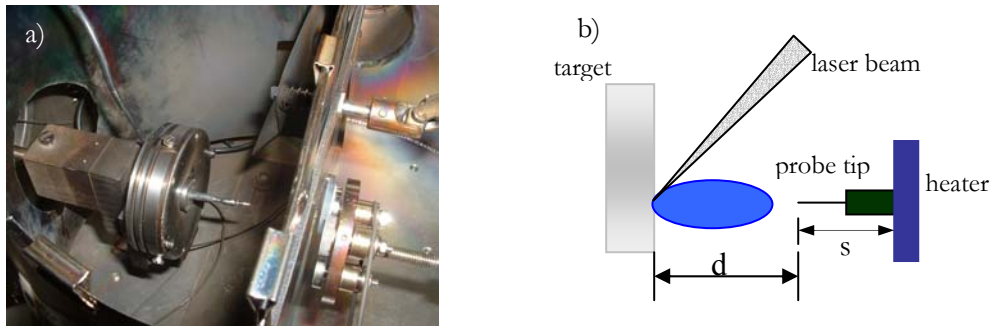


Figure 3.2: Picture (a) and schematic view (b) of the ion probe set up.

The ion-current to voltage transformation occurs in a so-called Koopman circuit (figure 3.3 a)). This simple circuit consists of a charged capacitor, which causes a voltage drop as a result of the collected ion current. A Tektronix TDS-210 Digital Oscilloscope connected to a PC by a RS-232 serial port performs the data acquisition. This oscilloscope is triggered by the “sync out” signal of the laser. The oscilloscope averages probe output signals over 16 TOF measurements since the signal is not very stable as a result from plasma instability. This instability is a result of laser instability and non-uniformity of the target material. Deposition of platinum on the probe tip does not influence the signal over time during experiments.

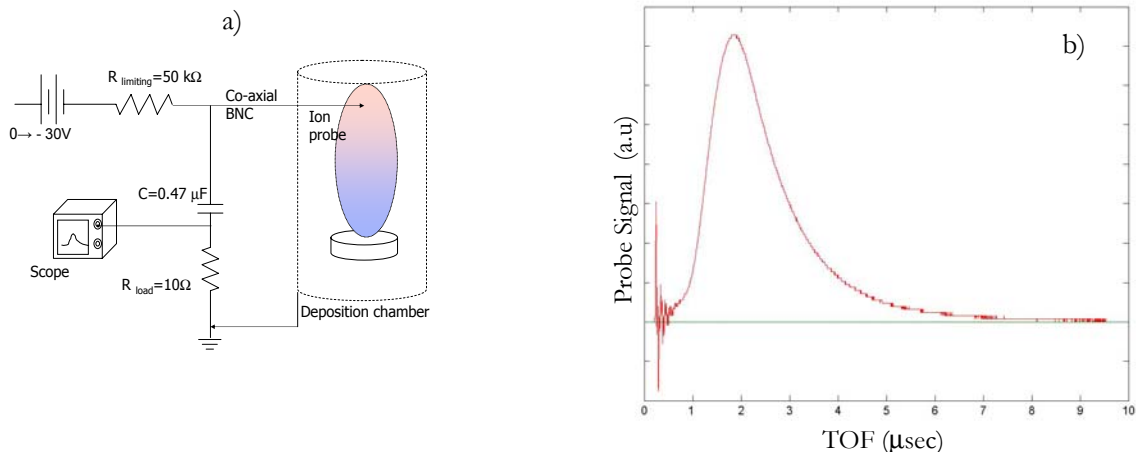


Figure 3.3: a) Koopman circuit and b) typical probe signal as a function of time

A typical output signal is shown in figure 3.3 b). The small peak of photoelectrons produced by Vacuum-Ultra Violet (VUV) light emitted from the ablated plasma enables $t=0$ to be determined from the TOF spectrum [9]. Since the probe tip is at a known distance, this TOF curve can easily be converted into a velocity distribution function. It should be noted that in this way *average* velocities are calculated.

3.3 Results

The first experiments done with the ion-probe were two series at different pressures with the distance as a variable. Pressures were chosen to be 0.1 and 1 mbar and the distance d started at 5 mm increasing with steps of 2.5 mm up till the signal became too small to measure. It is expected that with increasing distance the maximum probe signal will decrease due to expansion of the plasma and that the “dead time” will increase. The “dead time” is the period between the laser pulse and moment when the first and therefore fastest ions will reach the probe. Since at higher pressures the ions are more decelerated it is also expected that higher pressures will increase the dead time. The influence of the pressure on the maximum probe signal is not obvious since “slower” plasmas will give more time for the ions to recombine causing a decrease of the signal. The plasma is also more confined causing higher ion densities around the probe tip resulting in a higher probe signal.

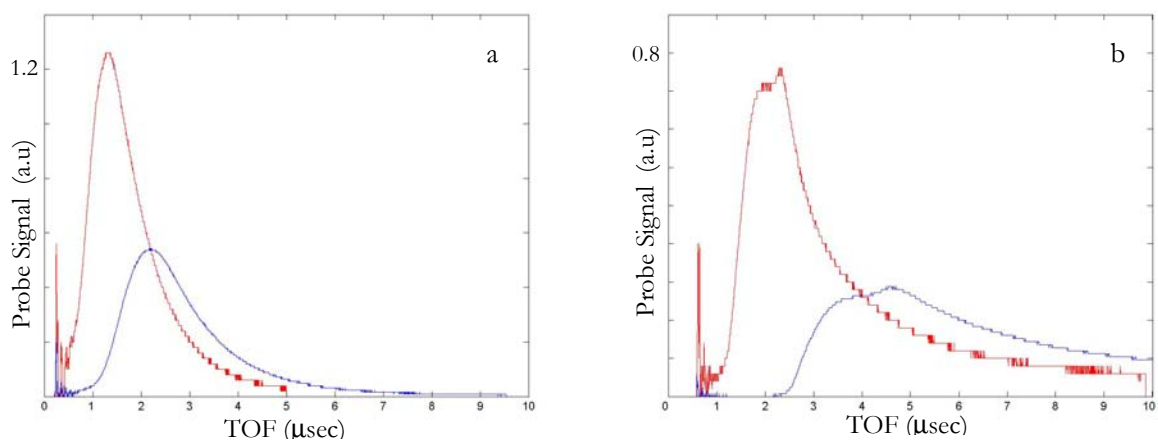


Figure 3.4: Measured time-of-flight curves for a) 0.1 mbar and b) 1.0 mbar. Each figure shows the probe signal as a function of time for two different distances d . The red curves are measured at a distance of 5 mm, the blue curves at a distance of 12.5 mm.

Figure 3.4 shows indeed a Maxwell shaped curve, an increase in dead-time with increasing distance and therefore seems to meet the first expectations. The bump in the TOF measurement in the right graph cannot be easily explained. This bump starts to appear at high pressures and has probably to do with the shockwave arising at these pressures. It is also observed that the maximum signal is lowered with increasing pressure as a result of fewer ions. These curves can now be transformed into a velocity distribution function since the distance and $t=0$ are well defined. This transformation to particle velocities results into the curves shown in figure 3.5. MB-fitting can also be carried out resulting in the black curves of figure 3.5. This MB-fit is made by adjusting the parameters a , s and v_0 of equation 3.3 independently until the best fit is obtained.

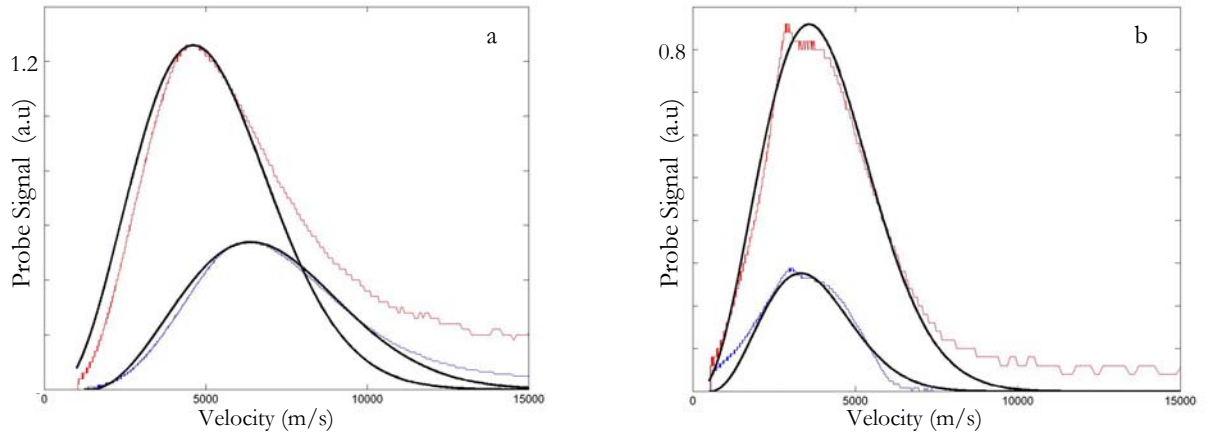


Figure 3.5: Velocity distribution function at a) 0.1 mbar, 5 mm (red curve) and 12.5 mm (blue curve) and b) 1 mbar, 5 mm (red curve) and 12.5 mm (blue curve). The Maxwell Boltzmann fit is included in black.

The MB-fit can be done ^[10] but they start to deviate at high velocities. This deviation might be a result of 2 different mechanisms. First, this might be caused by an incorrect response of the probe at high frequencies. More likely however, would be that high-energy ions on the edge of the plasma do not participate in the collision process in the Knudsen layer for the development of the “MB-gas”. These ions move undisturbed towards the probe and will cause higher signal at high velocities. At higher pressures and distances the ambient gas will decelerate these ions, lowering the tail of the distribution. This can be concluded since this deviation is pressure and distance dependent what would not be the case in probe response deviations. Other smaller differences between fit and data might have several causes. First of all, the assumption that the creation of the plasma is truly thermal is questionable. Secondly, only ions are measured so the curve does not describe the velocity distribution for all particles. Since ions are more energetic than their neutral atoms, a velocity distribution deviating from the one describing the complete plasma (including neutrals and clusters) will result. Finally it should be noted that the assumption has been made that every ion that was measured was singly ionized ^[10], double ionized particles will be counted for 2 singly ionized ones.

The parameters a , s and v_0 used to make the fit in figure 3.5 are given in table 3.1. Now the energy can be calculated by equation 3.5. The mass of a Pt ion is $3.24 \cdot 10^{-22}$ gram.

p (mbar)	d (mm)	a (kg/eV)	v_0 (m/s)	s	E (eV)
0.1	5	$5.0 \cdot 10^{-8}$	350	$8.4 \cdot 10^{15}$	30.4
0.1	12.5	$4.0 \cdot 10^{-8}$	1400	$6.8 \cdot 10^{15}$	38.0
1	5	$8.5 \cdot 10^{-8}$	150	$2.4 \cdot 10^{15}$	17.9
1	12.5	$1.3 \cdot 10^{-7}$	550	$3.3 \cdot 10^{14}$	11.7

Table 3.1: Fitting parameters for the fitted velocity distributions of figure 3.5.

The complete set of fitting parameters and particle energy can be plotted as a function of distance. This is shown in figure 3.6.

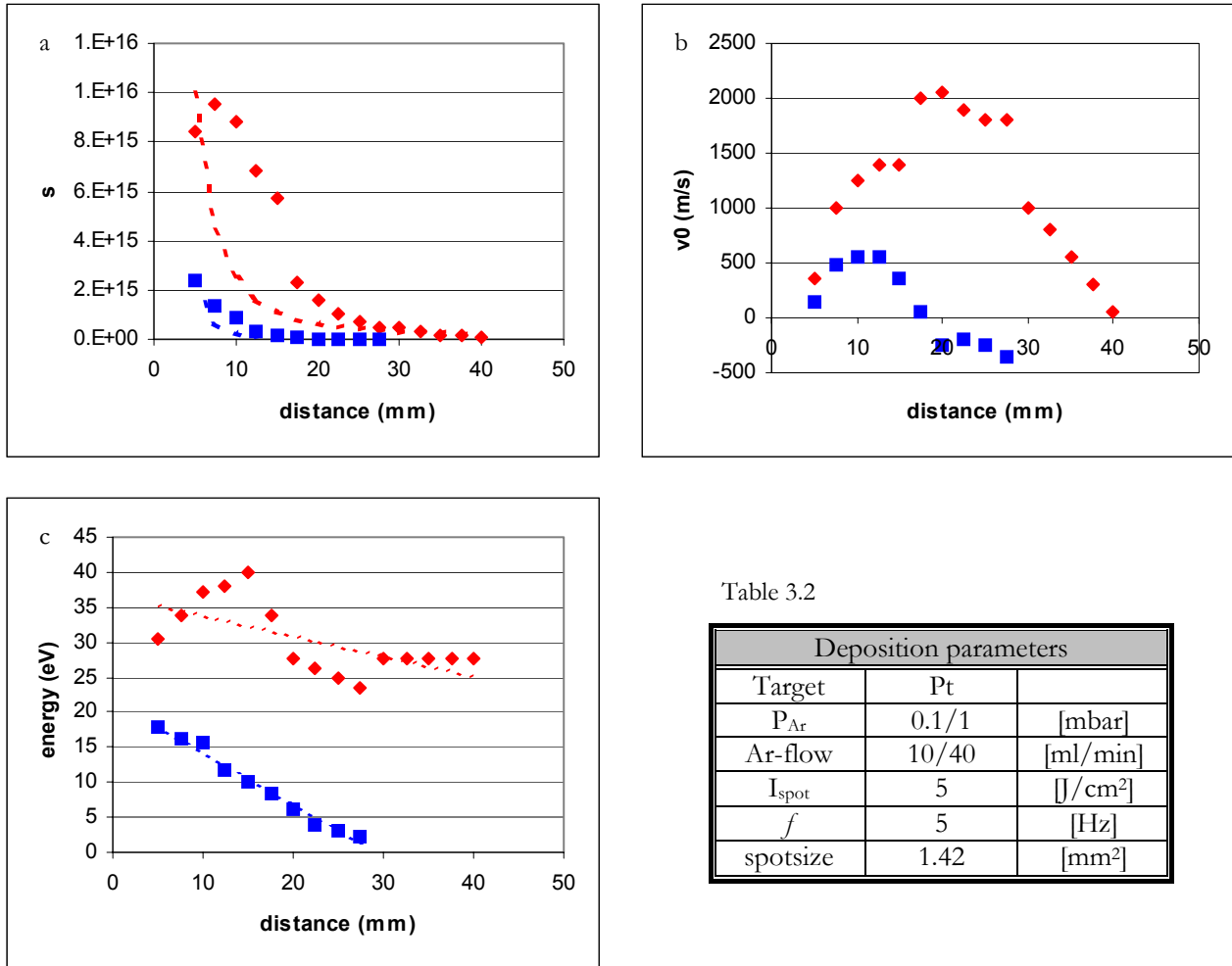


Table 3.2

Deposition parameters		
Target	Pt	
P_{Ar}	0.1/1	[mbar]
Ar-flow	10/40	[ml/min]
I_{spot}	5	[J/cm ²]
f	5	[Hz]
spotsize	1.42	[mm ²]

Figure 3.6: a) and b) fitting parameters s and v_0 as a function of distance and c) the calculated particle energy. The 0.1 mbar experiments are represented by the red data, the 1 mbar experiments by the blue data. The table 3.2 shows the deposition parameters.

The other important parameter influencing particle energy is the pressure. The same experiments as mentioned earlier can be done as a function of pressure. In figure 3.7 the particle energy measure by the ion probe as a function of pressure is depicted. An overview of the influence of the different deposition parameters on particle dynamics will be given in the next chapter.

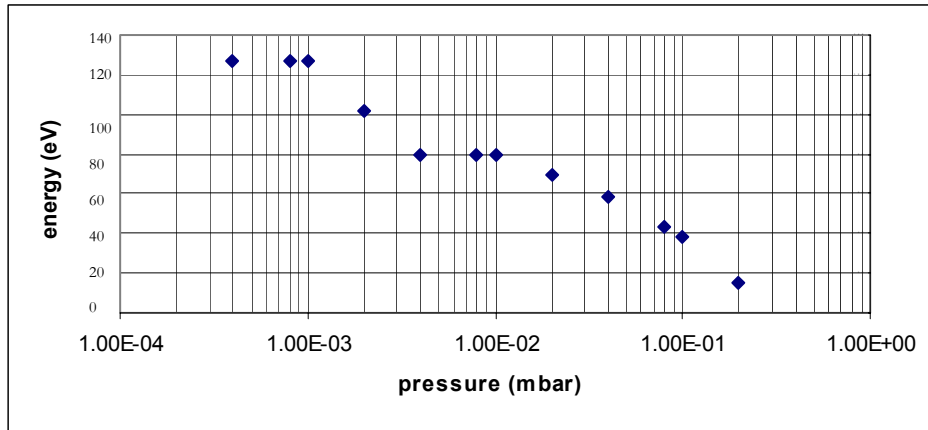


Figure 3.7: Measured particle energy as a function of pressure. The probe was positioned at 35 mm.

3.4 Discussion

From the measurements done with the probe several results showed interesting information about the laser-induced plasma.

Figure 3.6 a) shows a decrease in height of the probe signal. Since the plasma is not expanding from a point source, but forwardly peaked, the decay of this parameter is not proportional with $1/r^2$ (represented by the dashed line). The energy of the particles is indeed depending on the distance and pressure. At higher pressures, the energy is initially lower and drops faster as a function of distance. Interesting is the increase of the center of mass velocity at small distances. This implicates that the “plasma-cloud” is still accelerating ^[11] at small distances. This COM velocity goes to zero at larger distances. It even becomes negative for the 1 mbar experiment. This might be explained by the presence of the heater-plate behind the probe, reflecting the ions backward. Figure 3.7 shows a decrease in particle energy but the transition from the drag-force regime to the shock-wave regime cannot be found by these experiments. This might be a result of the relatively short distance of 35 mm compared to the work done by others ^[12].

3.5 Conclusion

The homemade Langmuir probe in combination with the electronic Koopman circuit worked at different pressures and target-substrate separations. Several trends in measured signals agreed with the expectation. Ion energies can be estimated as long as the probe collects enough ions. This becomes a problem at large distances and high pressures as can be seen in figure 3.6. At 1 mbar the signal becomes immeasurable at a distance of 35 mm. At 0.1 mbar this distance increased to 45 mm. For the deposition parameters used for “normal” deposition of thin films this is not a problem. For the deposition at high pressures and large distances another probe design can be used. By positioning the Koopman circuit near the probe, a voltage signal can be transferred along the coaxial cable instead of the small ion current. Also the use of a current amplifier will help at low signals.

Again, it is important to remind that the energy values are just an indication. It seems that the measured energies are in the right order of magnitude but a value for the accuracy is difficult to give. The largest error arises from the MB-fit to the probe signal since this has to be done manually. Assuming that the probe and electronics did not induce any error, several other processes can cause deviations. First of all, the measured ions do not form a real Maxwell-Boltzmann gas. The MB-fit is used as an energy estimate. Also ions reflecting from the heater will cause deviations. These reflected ions can be removed by removing the heater but taking these ions into account is useful since this simulates the real case of a substrate deposition.

Ion probe measurements can be very helpful for better understanding the particle dynamics of the pulsed laser produced plasma. Although it is not possible to extract accurate values for particle energies, it is possible to compare measured values obtained with different deposition parameters. Two velocity distribution functions can tell in one look what the influence of, for example, another mask geometry is.

4.1 Theory

According to the definition of the word “nano”, a nanoparticle is a cluster of material smaller than 100 nanometer in all three dimensions. At these particle sizes, a lot of the chemical and physical properties of materials start to deviate from bulk material. For certain applications, these changes in properties might be useful and a better control of particle size will be crucial. Also, films consisting of stacked nanoparticles can have other properties than thin (epitaxial) films.

For example, platinum nanoparticles find their application in altering the dielectric properties of materials, like dispersed nanoparticles in PZT, and in creating extreme porous conducting metal electrodes. A complete investigation of the growth kinetics of these platinum nanoparticles will result in better understanding of the formation process and ultimately in better control of particle size.

Pulsed laser deposition is a very suitable technique for nanoparticle growth studies due to its wide range of adjustable deposition parameters. For this research the ability to deposit at high pressures and obtaining high supersaturation ratios makes PLD a good candidate.

Nanoparticles can be formed by two different mechanisms [12]. The first is substrate growth. Particles from the plasma can nucleate at the surface of the substrate and due to the high mobility of the species arriving from the plasma island growth will result nanoparticles. The kinetic energy of the species arriving at the substrate is not high enough to form a thin film. These particles will grow in size until the substrate is covered and the process will proceed with columnar growth. The second growth mechanism is gas-phase nanoparticle formation. Due to the high supersaturation when the plasma is expanding, high nucleation rates can be obtained. Since the rate of homogeneous nucleation is strongly dependent on the saturation ratio, according to the classical condensation theory, particles with small critical radii can be formed. These particles travel towards the substrate and will be collected without any further substrate growth. These two growth modes are schematically depicted in figure 4.1.

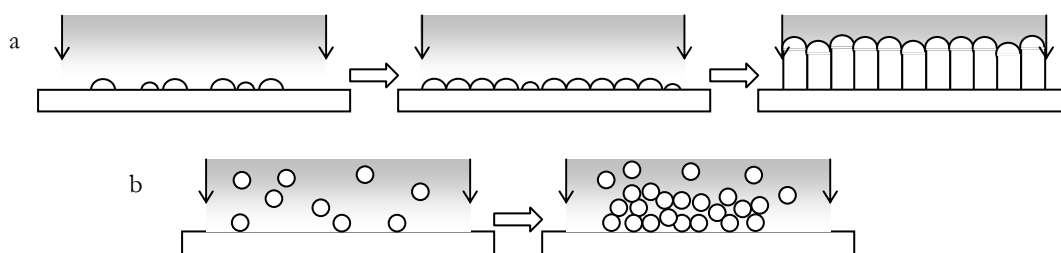


Figure 4.1: two different growth mechanisms for nanoparticle formation, from left to right longer deposition time. a) Atoms arrive at the substrate forming islands and eventually columns and b) fully developed particles arrive and stack at the substrate.

In this research, most attention is focussed on gas-phase nanoparticle formation. The growth of these nanoparticles under the extreme condition of PLD cannot be described by the classical condensation theory. But it is still important to note the basics of the formation of small particles out of a supersaturated vapour [13][14].

The free energy of formation of a condensate is determined from a balance between bulk cohesive forces between the atoms and a certain barrier due to surface tension. The Gibbs free energy to form a spherical condensate can be written in these two terms,

$$\Delta G(r) = -\frac{4}{3}\pi r^3 (n\Delta\mu) + 4\pi r^2 \sigma, \quad (4.1)$$

where $\Delta\mu = kT \ln(P/P_0)$ is the supersaturation, n is the atom number density and σ is the surface tension of the spherical droplet. So the free energy is lowered by the volume term and raised by the surface term. This free energy equation displays a maximum at a certain critical radius r^* ,

$$r^* = \frac{2\sigma}{n\Delta\mu}. \quad (4.2)$$

Nucleus sizes above this critical radius will grow further while smaller particles will decay, provided the solid or liquid phase is thermodynamically stable ($\mu_s, \mu_l < \mu_g$).

Since ions are present in the plasma it is important to note the influence of ions on the formation of nanoparticles [15]. Charged ions tend to be jacketed by neutral atoms if the medium consists of a dielectric material. The electric field surrounding the ions causes polarization of the dielectric material and as a result a minimum energy state exists. The critical radius r^* shifts as a result to a lower value. The expression for the free energy becomes,

$$\Delta G(r) = -\frac{4}{3}\pi r^3 (n\Delta\mu) + 4\pi r^2 \sigma + \left(1 - \frac{1}{\epsilon_c}\right) \left(\frac{Q}{8\pi\epsilon_0}\right) \left(\frac{1}{r} - \frac{1}{r_a}\right), \quad (4.3)$$

where ϵ_c is the dielectric constant of the material, Q is the ionic charge (mostly singly ionised in plasmas created by excimer lasers) and r_a is the radius of the jacketed ion. This term lowers the energy barrier substantially.

According to the classical condensation theory it can be concluded that the presence of a high degree of supersaturation and the presence of ions will lower the critical radius for particle formation. Even homogeneous- or self-nucleation can take place if supersaturation ratios are high enough. These requirements for the formation of nanoparticles are met in the PLD process. So it should be possible to create an environment where nanoparticle formation does take place.

As soon as particles are formed with a radius above the critical radius, the high degree of supersaturation in the plasma will result in a high deposition rate on these newborn particles according to [16],

$$\Delta\mu = k_B T \ln\left(\frac{R}{R_0}\right) \quad (4.4)$$

where k_B is Boltzmann's constant, R is the actual deposition rate and R_0 is the equilibrium deposition rate at temperature T . As the plasma is expanding more the supersaturation is eventually lowered over time. This causes lower deposition rates and an increase in critical radius. As a result some particles will disappear again by this increase in r^* .

Concluding, the high degree of supersaturation does not only create the possibility for particle formation by lowering the r^* but also fixes the deposition rate and consequently the final particle size.

4.2 Experimental

Experiments have been done under different deposition conditions. Since there was a lot of difficulty with analysing the samples it was not possible to extract exact values for the particle size. Comparing results of different sets of experiments was consequently not possible so experiments had to be done in series to minimize the effect of changes in the analysis. In this way comparison in changes in particle size and growth mode is possible. This chapter will discuss the influence of the different deposition parameters one by one. The significance of each parameter can be derived from these experiments.

4.2.1 The influence of target-substrate separation

It was found early on in the research that the target-substrate separations together with ambient gas pressure are the most important parameters influencing the growth mode and particle size. Figure 4.2 shows the AFM images of experiments done at a target-substrate separation of 35, 40 and 50 mm. At this pressure the substrate was placed outside the visible plasma and the substrate was kept at room temperature (RT).

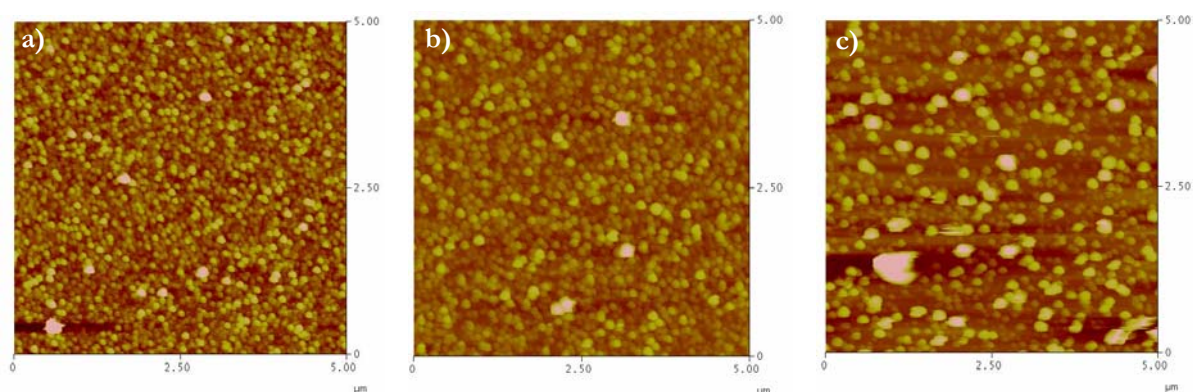


Figure 4.2: AFM images of deposited Pt nanoparticles in 1.6 mbar argon at 5 Jcm^{-2} and a laser repetition rate of 5 Hz as a function of target-substrate separation a) 35 mm (mean height 6.1 nm), b) 40 mm (mean height 11.3 nm) and c) 50 mm (mean height 28,6 nm).

The mean height increased with increasing target substrate separations. Also the roughness of the samples increased. As the separation becomes larger the particles formed in the plasma stay in the plasma for a longer period. Particles can grow for a longer time in this supersaturated environment before they are collected on the substrate. The increasing roughness is probably a result of the decrease in kinetic energy of the nanoparticles. With lower energies the particles are more “loosely” stacked. The increase in particle size with increasing distance is an indication for gas-phase growth. Increasing the separation will lower the kinetic energy of the species present in the plasma due to interaction with the ambient gas. The diffusivity on the surface is lowered resulting in smaller particles. Even at pressures above 1 mbar, substrate growth cannot be ruled out. It is possible to have no or hardly any nanoparticles formed in the supersaturated environment of the plasma at small distances from the target. If the substrate is placed in this range, substrate growth is induced resulting in columnar growth. This is depicted in figure 4.3 a). This experiment was done at 2 mbar of argon with a target-substrate separation of 36 mm.

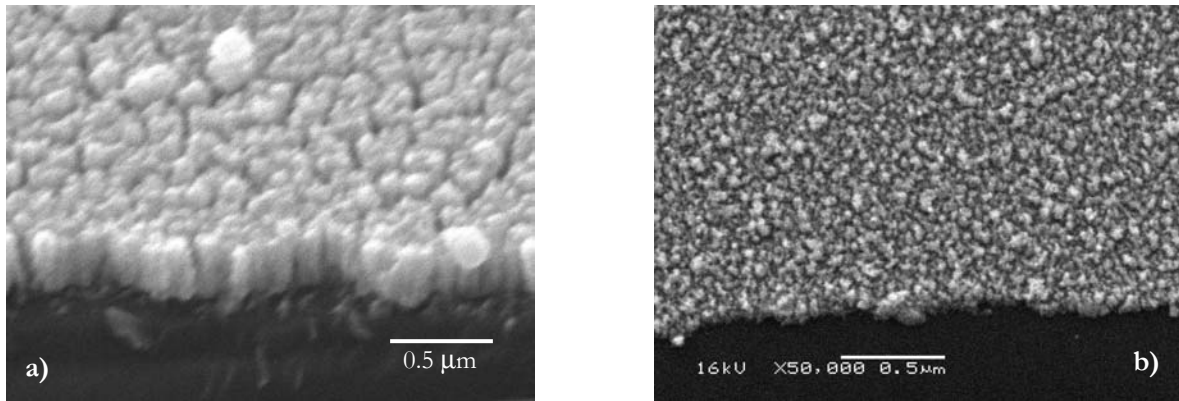


Figure 4.3: a) SEM image of Pt columns grown at 2 mbar of argon, 36 mm target-substrate separation and 5 Jcm^{-2} . b) SEM image of Pt nanoparticles grown at 1.6 mbar of argon, 45 mm target substrate separation and 5 Jcm^{-2} .

Figure 4.3 b) shows that columnar growth is eliminated by increasing the distance from 36 to 45 mm. Pressure seems to be of less importance to get rid of substrate growth. The formation of a smooth metallic platinum film did not occur at any distance at pressures higher than 1 mbar.

At even larger target-substrate separation ($> 60 \text{ mm}$) hardly any nanoparticles could be detected. Figure 4.4 shows SEM images of experiments done at target-substrate separations of 90 and 60 mm. Particles cluster together probably already in the gas-phase creating larger structures (figure 4.4 b) and only the structures with enough kinetic energy will reach the substrate (figure 4.4 a). These large clusters are not observed at separations smaller than 60 mm. Depositions are not effective any more at these distances since hardly any particles reach the substrate.

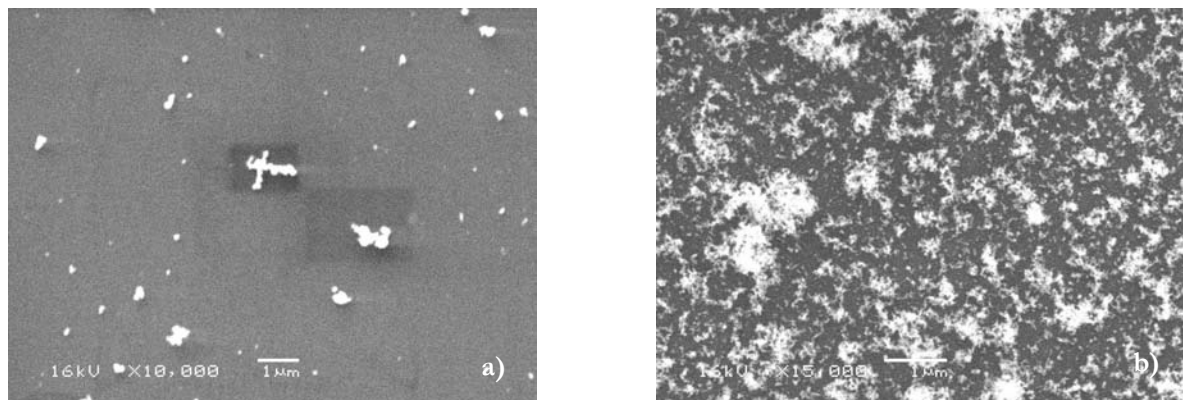


Figure 4.4: SEM image of Pt clusters formed at target-substrate separations of a) 90 mm and b) at 60 mm. Other parameters were 1.6 mbar of argon and 5 Jcm^{-2} laser fluence.

4.2.2 Influence of the ambient gas pressure

The other important parameter for nanoparticle formation was expected to be the process pressure. A high degree of supersaturation can be obtained by sufficient cooling of the expanding plasma. At higher background pressures, the plasma can be cooled more effectively while it is contained in a small volume. As a result it is expected to obtain larger nanoparticles at higher pressures.

Pressure during the depositions was measured with a pressure sensor (MKS series 902) that is able to cope with the high pressures needed for particle growth. Pressures ranged from 1 to 10 mbar. Results of 4 different experiments done at 1.3, 1.8, 4.0 and 10.0 mbar are shown in figure 4.5.

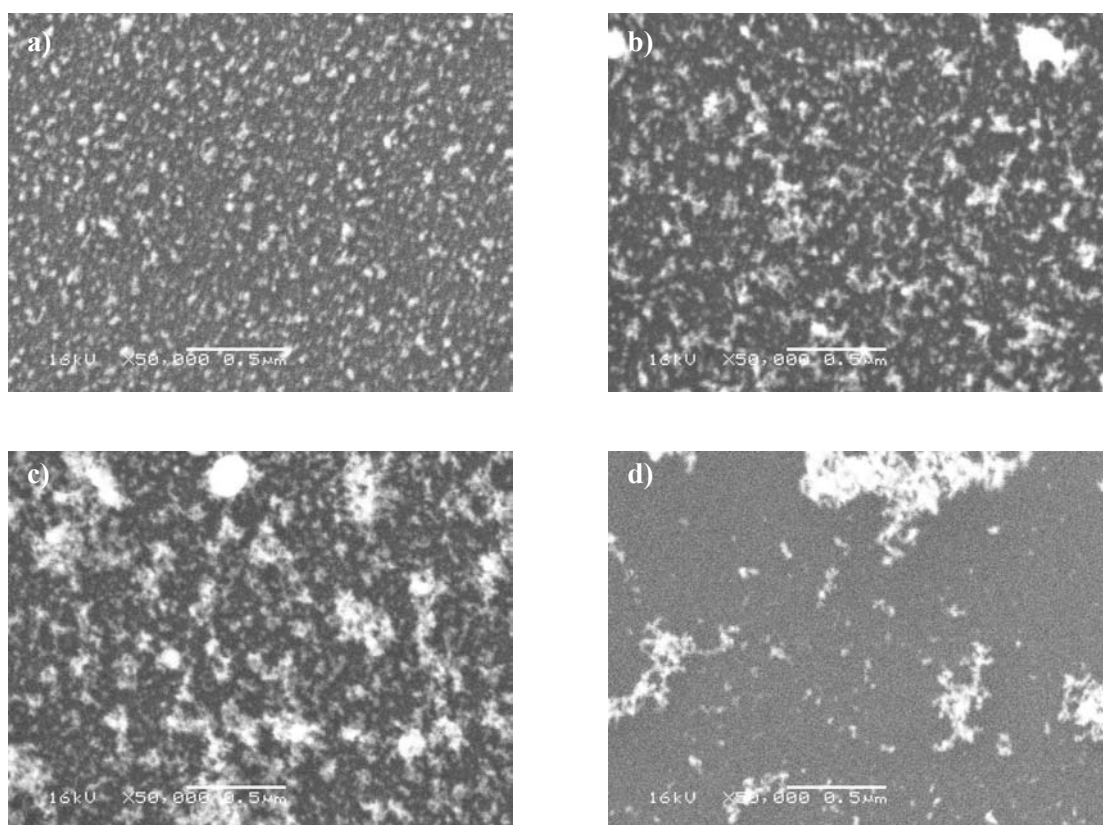


Figure 4.5: SEM images of experiments done in the pressure series. Argon pressure varied from a) 1.3 mbar, b) 1.8 mbar, c) 4.0 mbar and d) 10.0 mbar. Other deposition parameters were a deposition time of 15 minutes, fluence 5 Jcm^{-2} and target-substrate separation of 45 mm.

Particle sizes could not be obtained by AFM imaging due to extreme roughness and fragility of the samples. SEM images show larger structures with increasing pressure. At pressures between 1 and 2 mbar and a target-substrate separation of 45 mm homogenous gas nanoparticle formation was obtained. At higher pressures particles seem to form larger clusters up to several microns at 10 mbar. These clusters “hover” in the deposition chamber for several seconds. This can be observed by the naked eye when the next laser pulse strikes these clusters. Lowering the pressure did not result in substrate growth but pressures <0.1 mbar resulted in film growth.

4.2.3 Influence of spot size and spot geometry

By slightly increasing the spot size the shape of the plasma is unchanged. The only difference is that more particles are being ablated from the target, resulting in higher number densities. So it is expected that particles will grow with increasing spot size. An experiment has been carried out to investigate this by increasing the spot size with $\sim 40\%$. Other deposition parameters were kept constant. As far as it can be observed by the naked eye, the visible plasma did not grow with increasing spot size. The results were analysed by SEM and are shown in figure 4.6.

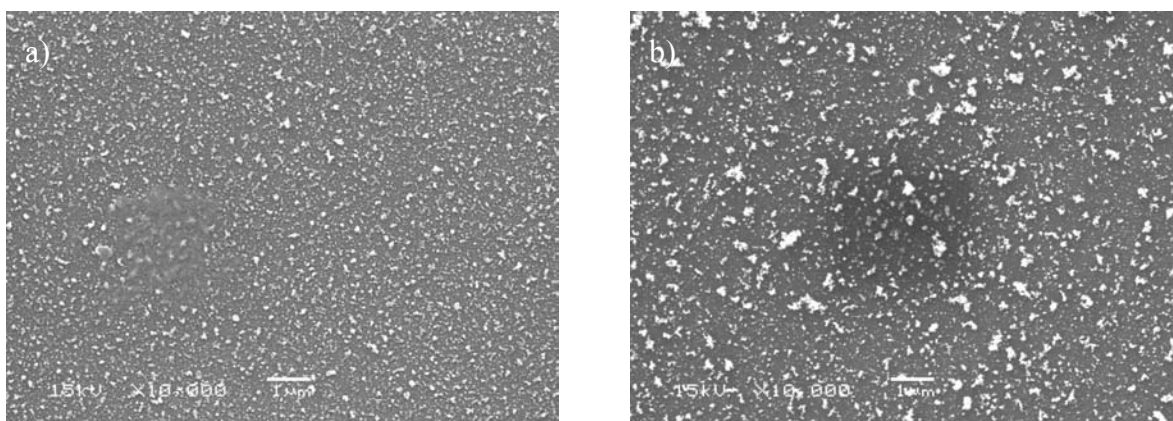


Figure 4.6: SEM images for a) nanoparticles grown with a spot size of 1.03 mm^2 and b) 1.42 mm^2 . Other parameters were a fluence of 5 Jcm^{-2} , deposition time of 4 minutes, target-substrate separation of 45mm and a argon pressure of 1.6 mbar.

The SEM images show an increase in particle size with increasing spot size. Larger clusters are also formed with the larger spot size. This might be a result of the higher supersaturation as shown in paragraph 4.2.2 or a result of stacking of particles as will be explained in paragraph 4.2.5.

The influence of the spot geometry is more complex than the spot size or other deposition parameters. For this research a very narrow slit ($1 \times 15 \text{ mm}^2$) is selected instead of the usual 55.9 mm^2 rectangular mask. The plasma will become broader in the x-y plane (parallel with the target) and shorter in the z direction (the created plasma approaches a plasma formed from a “point source”). This plasma shape has a relatively larger area that can be cooled more effectively. Another consequence of this other spot geometry is the resulting spot size, which is roughly 5 times smaller, resulting in less ablated material. The influence of this other mask is shown in the AFM image in figure 4.7.

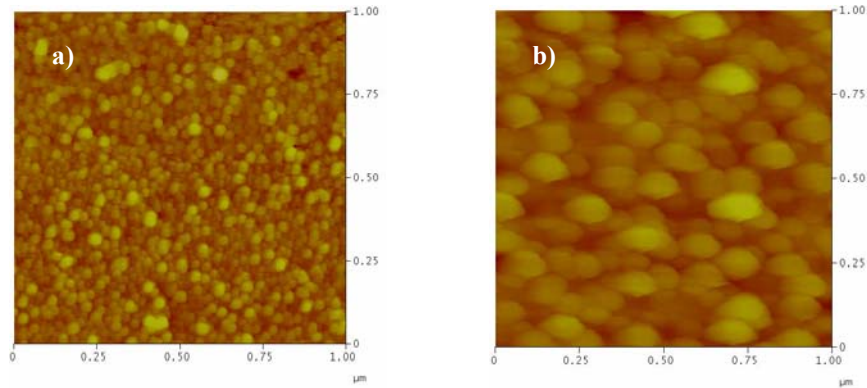


Figure 4.7: AFM images showing the influence of different spot geometries. a) Particles formed with the $1 \times 15 \text{ mm}^2$ mask, fluence 5 Jcm^{-2} , target substrate separation 45 mm and a spot size of 32 mm^2 . b) Particles formed with the 55.9 mm^2 mask, spot size of 1.44 mm^2 , other parameters were kept the unchanged.

This other spot geometry resulted in much smaller particles. The lower number density probably lowers the supersaturation. This is the result of less particles from the smaller spot size in a relatively big spherical shaped plasma. The particles formed are still larger than substrate grown particles.

4.2.4 Influence of the laser repetition rate

At first glance the laser repetition rate does not influence the supersaturation or the kinetic energy of the ablated species. Nevertheless above a certain repetition rate particles notice the presence of the remains of the previous pulse. It can lower the interaction of the ablated species with the background gas. This can be a result of particles “tunnelling” in the wake of the preceding pulse [12]. Consequently the cooling of the plasma will be less and the kinetic energy of the particles will be higher. An experiment done at a repetition rate of 40 Hz , SEM image is given in figure 4.8, showed that even a columnar like growth could be obtained where at the normal repetition rate particle growth was observed (figure 4.3 b).

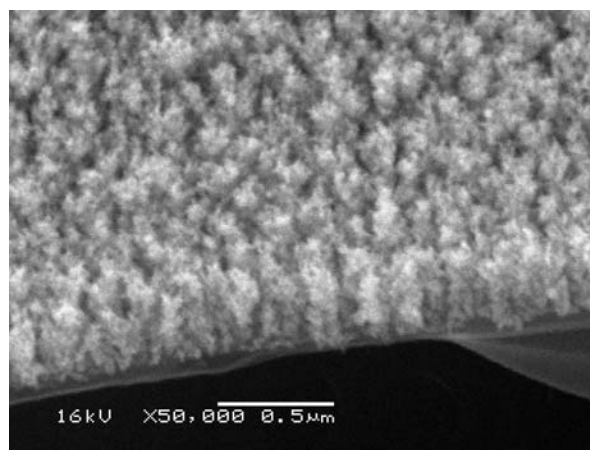


Figure 4.8: SEM image of Pt deposited at a laser repetition rate of 40 Hz , $1,6 \text{ mbar}$ of argon, 45 mm and 5 Jcm^{-2} . The deposited material is not particle like nor is it truly columnar grown.

For gas phase nanoparticle formation the laser repetition rate should not be too high, 5 Hz seems to be a proper value. To diminish the interaction between material left over from the preceding plasma and the next one, even lower frequencies might be chosen. Other work [14] showed that material could hover between target and substrate up to 20 seconds.

4.2.5 Influence of the deposition time/number of pulses

The deposition time will not influence the nanoparticle size for truly gas phase nanoparticle formation since no substrate growth is present. In case of substrate nanoparticle formation, an increase in the number of laser pulses could produce evidence for substrate growth. The particle size will then increase with increasing number of laser pulses. Several experiments have been performed to get more insight in the formation process as a function of deposition time.

First, depositions were carried out at 0.5, 1.0, 2.0 and 4.0 minutes under the conditions of gas phase nanoparticle formation. These samples were analysed by SEM and are shown in figure 4.9 a). Secondly, depositions were done for only 6 and 30 pulses at a target substrate separation of 36 mm. Now substrate growth is expected as shown in paragraph 4.2.1. These samples were analysed by AFM and are shown in figure 4.9 b).

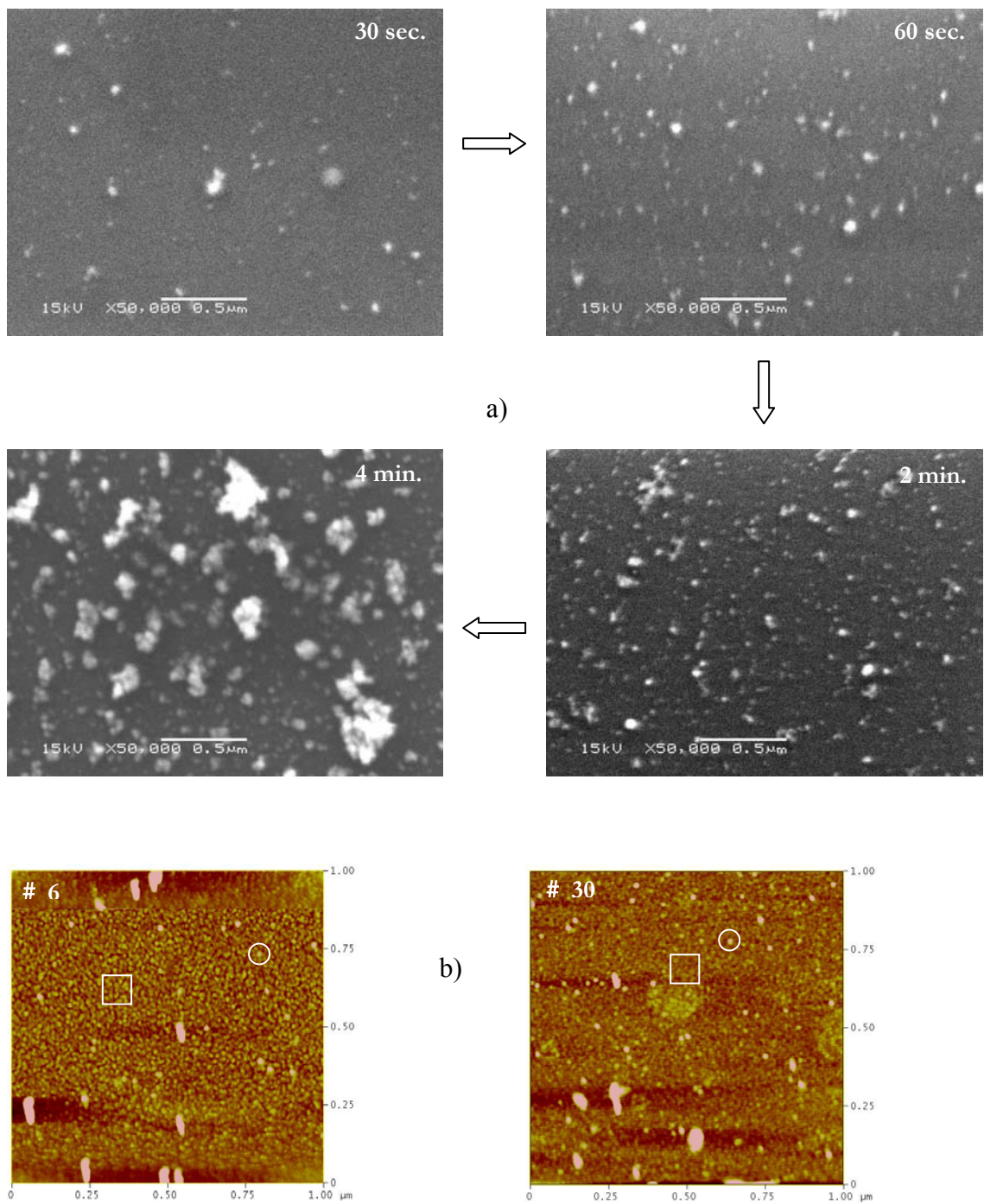


Figure 4.9: a) SEM images of nanoparticles formed in the gas-phase for increasing deposition times. Other deposition parameters were laser fluence of 5 Jcm^{-2} , target-substrate separation of 45 mm and 1.6 mbar of argon. b) AFM image of nanoparticles formed on the substrate/gas-phase for 6 and 30 pulses, 5 Jcm^{-2} , 36 mm and 1.6 mbar of argon. The circles indicate gas-phase particles, the squares groups of columns.

Figure 4.9 a) indeed shows an increase in the number of particles. Up to 2 minutes of deposition time the number of particles increases and for longer deposition times the particles are stacked more and more. There is no significant increase in particle size. Figure 4.9 b) indicates that at a target-substrate separation of 36 mm both growth modes coexist. The white squares indicate columnar growth and the white circles select a gas-phase grown particle. The number of gas-phase grown particles increases as well as their size with increasing number of pulses. These particles are several times larger than substrate grown particles. Larger particles on top of a structure of columns have also been observed in the target-substrate separation experiments.

4.3 Deterioration of Pt-nanoparticle films

Early on in the research it appeared that the produced samples deteriorated over time. First indications arose when SEM imaging became more difficult after several days and even impossible after a week. This might be a result of oxidation of platinum. The huge surface of stacked nanoparticles could result in noticeable oxidation, although platinum hardly reacts with oxygen under normal circumstances. Most common Pt oxides are PtO and PtO₂. These compounds decompose at 325°C and 450°C [18] respectively. So, by heating the samples, the oxygen can be removed. Although Pt melts at 1768°C it might be possible that the nanoparticles turn into larger structures at lower temperatures as a result of some sintering process.

It was also observed that Pt-nanoparticle films attract water and retain it inside the structure. This became clear by AFM imaging. A droplet, growing with scanning time, was formed at the tip and drawn along the surface of the sample. The optical microscope mounted on the AFM can observe the growth of this droplet. When the tip is withdrawn from the surface, a droplet is left behind which is again completely absorbed by the structure in several seconds. By heating the sample this water will disappear.

This deterioration of the samples won't be a problem in oxygen/NO_x sensors, since these operate at temperatures much higher than 450°C.

4.4 Discussion

Different experiments led to insight in the influence of different parameters on nanoparticle formation in the PLD process. The influence of the different parameters agreed to a certain extent with the expectations from theory about supersaturation. A very difficult parameter to predict is the spot geometry since it influences several circumstances in the process at the same time, all having a positive or negative influence on the supersaturation.

As can be seen in the figures of this chapter, the quality of these images is not always as desired. Reasons for this are explained in chapter 1. Transmission Electron Microscopy (TEM) [19] is a non-interaction method with a high resolution that could solve the problems encountered with AFM and SEM.

In this work, all parameters were tested on their influence on nanoparticle formation. Experiments showed early on in the research two very important parameters, ambient gas-pressure and target-substrate separation. By setting these parameters, gas-phase nanoparticle formation can be obtained. Other parameters can be used to tune the particle sizes.

4.5 Conclusions

The main variable in nanoparticle formation, according to the classical condensation theory and deposition rate equations, is the supersaturation. Series of experiments showed that gas phase nanoparticle formation could indeed be explained by this one parameter. Each deposition parameter influences the supersaturation more or less. A high supersaturation ratio is obtained when two conditions are met. First, a large amount of atoms are needed in a confined space and secondly, the temperature of this 'gas' has to be lowered rapidly. It is quite hard to tamper with the first requirement for a high degree of supersaturation. The spot size can be altered but only by several percents without changing the shape of the plasma significantly. There are better ways to control the supersaturation. By changing the spot geometry, for example, the whole shape of the plasma is altered. A small "point source" will give a more spherical shaped and smaller plasma that can be cooled more effectively by the background gas compared to the generally known "ellipsoid". The influence on the supersaturation and consequently the particle size is hard to predict. The laser fluence influences the amount of particles emitted and the initial temperature but this is not investigated in this research. These are the parameters influencing the number density for the supersaturation mainly.

The ambient gas pressure seems to have a dual function. First, a high background pressure will result in a smaller plasma containing the same amount of species resulting in a higher number density. Secondly, the plasma is cooled more. Together, this will result in a high supersaturation. Finally, the target-substrate separation has a large influence on the particle size. This parameter does not influence the supersaturation but simply the time that particles spent in this supersaturated environment.

Gas-phase nanoparticles can indeed be grown by PLD although the parameter window is rather small. At low pressures (≤ 1 mbar) and small target-substrate separations (< 35 mm) substrate growth will take over. Extremely high pressures (> 3 mbar) and large target-substrate separations (> 60 mm) will create clusters of particles, resulting in micron-sized structures. If the correct regime is found in pressure and target-substrate separation, the size can be tuned by other parameters.

General Discussion and Conclusions

Up till now, nanoparticle formation and ion-probe results have been discussed separately. The primary goal of this kind of plasma diagnostics was to forecast whether the right regime for particle formation had started. Unfortunately, from the results shown in chapter 2 and chapter 3 it is obvious that the parameter windows do not match.

To measure an ion signal at the target-substrate separation used most, a pressure is needed well below 0.1 mbar and signals become immeasurable at 1 mbar when separations are larger than 30 mm. The regime for substrate particle growth does start under the deposition conditions that can be investigated by the ion probe. Since the start of substrate particle growth is not investigated in this work and no sudden changes in fitting parameters can be observed, it is not sure whether ion-probe measurements could indicate the substrate particle growth regime.

To overcome the problems, signal amplification near the probe can be done or another set-up to minimize current transport through a coaxial cable could be used. Anyway, the probe gave results in the regime where “usually” depositions are done, so this tool might be helpful in other research.

Figure 5.1 gives is a schematic graph for the results of different experiments done with the main parameters for nanoparticle formation, pressure and target-substrate separation. This picture also shows the limit, indicated by the blue line, where ion-probe measurements can be done. Above this line, no probe experiments can be done.

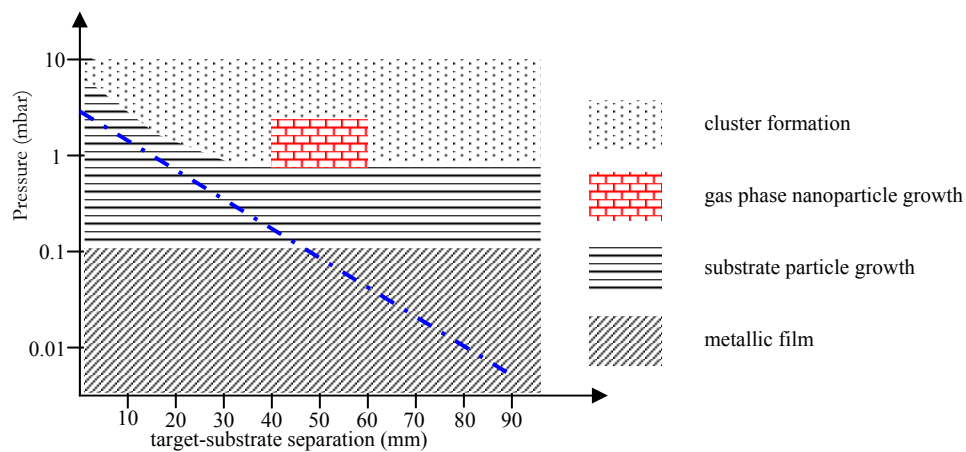


Figure 5.1: Schematic graph indicating the growth modes for nanoparticles as a function of pressure and target-substrate separation. The blue line indicates the limit for ion-probe measurements.

The red patterned area in figure 5.1 indicates the small window for homogeneous platinum nanoparticle growth in the PLD process. In this window, sizes can be tuned by changing other less rigorous parameters. For platinum, resulting particles will have a size in the order of tens of nanometers.

Dankwoord

Een verslag is geen verslag zonder dankwoord. Dit verslag was er überhaupt niet geweest zonder de mensen die ik graag wil noemen in dit dankwoord. Een onderzoek als dit is niet mogelijk zonder de steun en inzet van heel veel mensen. Hoewel de kans bestaat dat ik iemand vergeet, wil ik toch een poging wagen iedereen te bedanken voor zijn/haar inzet.

Allereerst natuurlijk Dave, niet zomaar de professor van de groep maar als sinds jaren een enorme inspiratiebron in mijn studie en helemaal in dit afstudeerwerk. Hetzelfde voor Guus, mijn “tweewekelijkse-en-loop-eens-binnen” begeleider, het is geweldig hoe jullie tussen neus en lippen door een ideetje uit de mouw schudden wat mij weer nieuwe inspiratie gaf om verder te gaan. En dan natuurlijk mijn dagelijkse (zeg maar uurlijkse) begeleider Frank, iemand die altijd tijd voor me had en anders wel vrij maakte. Ook wil ik Frank, Guus en “ons pa” bedanken voor hun inzet bij het verbeteren van mijn verslag.

Verder zouden alle experimenten niet gedaan kunnen worden door de hulp van Frank en Dick. Een idee kan nog zo mooi zijn maar zonder jullie is het praktisch niet te realiseren. Verder wil ik de mensen van de vakgroep IMS bedanken, bij wie ben ik niet binnen gevallen om eens wat te vragen.

Ook wil ik de studenten uit onze studententuin bedanken voor de vele fijne discussies. Niet alleen over wetenschap maar ook over welke woorden nou wel en niet kunnen in galgje. De nodige afleiding werd ook verzorgd door mijn minigolfmaatjes, waar ik geen namen van zal noemen, bedankt hiervoor. Voor verdere nodige afleiding tijdens mijn afstuderen, ook buiten werktijd, wil ik graag de Brak, Aico, Frank!, Dekkers, Ard en vele anderen bedanken. Natuurlijk mag ik ook niet mijn kleine broertje vergeten die op de meest onmogelijke momenten voor mij heeft klaar gestaan.

Als laatste wil ik mijn ouders bedanken, zonder hun steun was mijn studie niet eens mogelijk geweest, laat staan mijn afstuderen en natuurlijk mijn vriendin Tina, die door mijn afstudeerperikelen niet eens op vakantie kon.

Literature

- 1 D. B. Geohegan, A. A. Puretzky, G. Duscher and S. J. Pennycook, *Applied Physics Letters* **72** 23 p.2987-2989 (1998), *Time resolved imaging of gas phase nanoparticle synthesis by laser ablation.*
- 2 T. Orii, M. Hirasawa and T. Seto, *Applied Physics Letters* **83** 16 p.3395-3397 (2003), *Tunable, narrow-band light emission from size-selected Si nanoparticles produced by pulsed laser ablation.*
- 3 D. B. Chrisey and G. K. Hubler, *Pulsed laser deposition of thin films* (Wiley-interscience), 1994
- 4 G. Ding, J. E. Scharer and K. L. Kelly, *Journal of Applied Physics* **84** 3 p.1236-1240 (1998), *Effects of rapidly decaying plasmas on Langmuir probe measurements.*
- 5 T. N. Hansen, J. Schou and J.G. Lunney, *Applied Physics A*. **69** (1999) p.601-604, *Langmuir probe study of plasma expansion in pulsed laser ablation.*
- 6 D. W. Koopman, *The Physics of Fluids*, **14** 8 (1971) p.1707-1716, *Langmuir probe and microwave measurements of the properties of streaming plasmas generated by focused laser pulses.*
- 7 N. Hershkowitz, *Plasma probes*, Handbook of thin film process technology, **D3.0:1**
- 8 R. Kelly and R. W. Dreyfus, *Surface Science* **198** (1988) p.263-276, *On the effect of Knudsen-layer formation on studies of vaporization, sputtering and desorption.*
- 9 Oliver Kelly, www.maths.tcd.ie/~olly/wr1.pdf, (2000), p.6-9, *Production and characterization of amorphous carbon thin films by PLD.*
- 10 T. N. Hansen and J. Schou, *Applied Physics Letters* **72** 15 (1998) p.1829-1831, *Angle-resolved energy distributions of laser ablated silver ions in vacuum.*
- 11 F. Claeysens, A. Cheeseman, S. J. Henley and M. N. R. Ashfold, *J of Appl. Physics*, **92** 11 (2002) p.6886-6894, *Studies of the plume accompanying pulsed ultraviolet laser ablation of zinc oxide.*
- 12 L. Doeswijk, *Pulsed Laser Deposition of Oxides on Silicon: exploring their passivating qualities*, Ph.D. thesis, University of Twente, the Netherlands (2002).
- 13 Ivan V. Markov, *Crystal growth for beginners* (World Scientific) p.1-8/63-68 (1995)
- 14 K. C. Russell, *J. of Chem. Physics* **50** 4 p.1809-1816 (1969), *Nucleation on gaseous ions*
- 15 M. S. Tillack, D.W. Blair and S. S. Harilal, *Nanotechnology* **15** (2004) p.390-403, *The effect of ionisation on cluster formation in laser ablation plumes.*
- 16 A. J. H. M. Rijnders, *The initial growth of complex oxides: study and manipulation*, Ph.D. thesis, University of Twente, the Netherlands (2001).
- 17 R. Jordan and J. G. Lunney, *Applied Surface Science* **127-129** (1998) 968-972, *Investigation of excimer laser ablation of iron.*
- 18 www.webelements.com
- 19 A. G. Gnedovets, E. B. Kul'batskii, I. Smurov and G. Flamant, *Applied Surface Science* **96-98** p.272-279 (1996), *Particle synthesis in erosive laser plasma in a high pressure atmosphere.*